Article

Including Lifetime Hydraulic Turbine Cost into Short-Term Hybrid Scheduling of Hydro and Solar

Jiehong Kong [1,*] **, Igor Iliev** [2] **and Hans Ivar Skjelbred** [1]

[1] Department of Energy Systems, SINTEF Energy Research, Sem Sælands vei 11, 7034 Trondheim, Norway; hansivar.skjelbred@sintef.no
[2] Aker Solutions Hydropower AS, Oksenøyveien 8, 1366 Lysaker, Norway; igor.iliev@akersolutions.com
[*] Correspondence: jiehong.kong@sintef.no

Abstract: In traditional short-term hydropower scheduling problems, which usually determine the optimal power generation schedules within one week, the off-design zone of a hydraulic turbine is modeled as a forbidden zone due to the significantly increased risk of turbine damage when operating within this zone. However, it is still plausible to occasionally operate within this zone for short durations under real-world circumstances. With the integration of Variable Renewable Energy (VRE) into the power system, hydropower, as a dispatchable energy resource, operates complementarily with VRE to smooth overall power generation and enhance system performance. The rapid and frequent adjustments in output power make it inevitable for the hydraulic turbine to operate in the off-design zone. This paper introduces the operating zones associated with various production costs derived from fatigue analysis of the hydraulic turbine and calculated based on the turbine replacement cost. These costs are incorporated into a short-term hybrid scheduling tool based on Mixed Integer Linear Programming (MILP). Including production costs in the optimization problem shifts the turbine's working point from a high-cost zone to a low-cost zone. The resulting production schedule for a Hydro-Solar hybrid power system considers not only short-term economic factors such as day-ahead market prices and water value but also lifetime hydraulic turbine cost, leading to a more comprehensive calculation of the production plan. This research provides valuable insights into the sustainable operation of hydropower plants, balancing short-term profits with lifetime hydraulic turbine costs.

Keywords: accumulated damage; short-term hybrid scheduling; turbine cost; production cost; fatigue load

1. Introduction

Nowadays, hydropower, as a dispatchable energy resource, complementarily operates with Variable Renewable Energy (VRE) [1]. Although the hybrid system of hydropower and VRE can smooth overall power generation and enhance system performance, it also changes the operating pattern of hydraulic turbines. The rapid and frequent adjustments in output power, intended to offset the intermittency of wind and solar generation, can lead to increased hydraulic turbine wear [2]. Moreover, when a hydro producer participates in both energy and capacity markets, the optimal decision involves not only the generation schedule but also the reserved capacity for various types of ancillary services [3]. Environmental constraints, such as the minimum flow requirement on the downstream river, can also force the turbine to operate in a part-load region [4]. All these factors necessitate the operation of hydraulic turbines in off-design zones, thereby increasing the risk of fatigue damage.

The operation of a hydraulic turbine imposes different degrees of fatigue load on the turbine components, particularly the turbine runner. This fatigue load can lead to the formation of new microscopic cracks within the material and influence the growth rate of pre-existing flaws, ultimately resulting in a material failure over time. The lifespan

of a brand-new runner, until failure, depends on several factors, including the turbine's operating patterns and the runner's structural integrity [5,6]. Figure 1 presents a fatigue analysis for a hydraulic turbine, showing the probability of accumulated damage from continuous operation at various power outputs over one week. For example, operating at 21 MW for one week induces approximately 1% damage to the runner. Prolonged operation at this power level for 100 weeks can cause cracks, emphasizing the need to limit annual operation within this range to 300–500 h. If extended operation is necessary, the cost of potential premature damage should be included in the production cost of electricity generation.
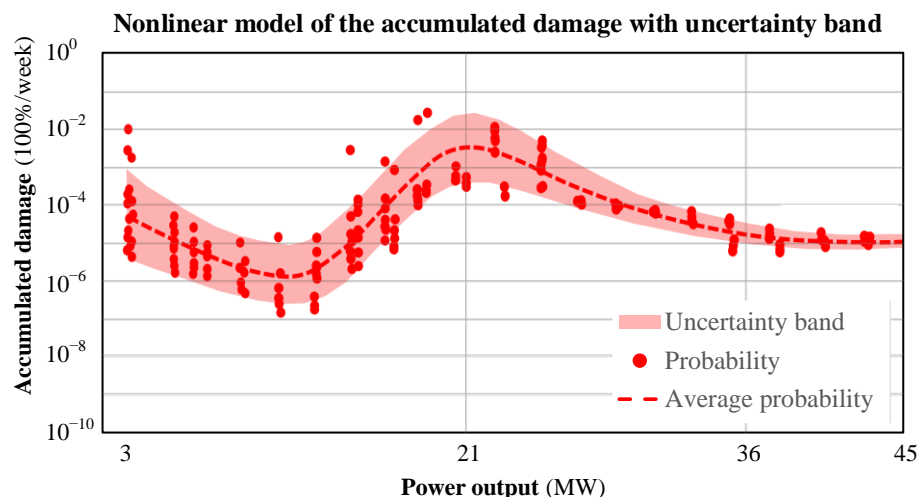

Figure 1. A typical fatigue analysis for a hydraulic turbine.

　　　Figure 2 illustrates a hill chart of turbine efficiency within the head-dependent operating range for single and multiple units. Hydraulic turbines are designed to achieve peak efficiency at a specific operating point on the hill chart, known as the design point or Best Efficiency Point (BEP). When operating near this point, turbines run smoothly and experience normal fatigue-related damage. However, operating further away from the BEP, referred to as off-design operation, will result in suboptimal flow conditions and increased pressure pulsations, both deterministic and stochastic in nature. Figure 1 indicates that operating at 36 MW near BEP results in smooth operation. One week of continuous operation at this level induces only about 0.001% damage, three orders of magnitude less than the damage from operating at 21 MW for the same duration.
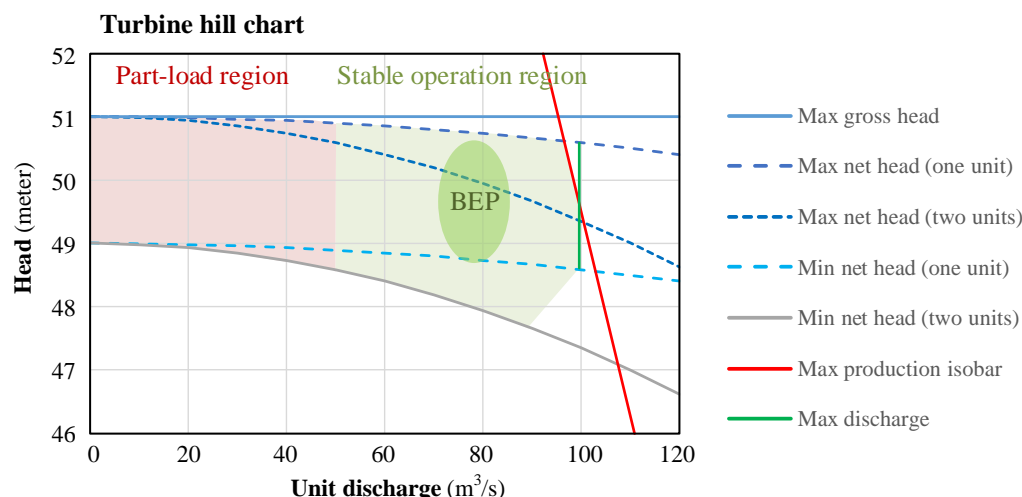

Figure 2. An example of the hill chart of a hydraulic turbine.

The fatigue analysis and the hill chart provide valuable insights into the turbine's durability and operational efficiency. A forbidden zone is an off-design operating condition where the turbine experiences high mean and fluctuating stresses, leading to significant fatigue loads. These zones depend on the turbine's hydraulic and structural design and are not always present. While it is possible to design turbines to operate under a high number of load cycles across the entire performance range without forbidden zones, not all current turbines in operation are designed this way. Therefore, it is crucial to avoid these zones whenever possible, operating within them only when necessary or economically justified.

Traditional short-term hydropower scheduling problems, which typically determine the optimal power generation schedules within one week, focus on precisely modeling forbidden zones and effectively incorporating them into the optimization problems. Medium- and small-sized units usually have a single, regularly shaped forbidden zone [7–9], while large-sized units possess multiple, irregularly shaped forbidden zones that vary with the head [10]. These zones can be approximated using several polygons [11] or triangulation techniques [12]. In the emerging field of multi-energy complementary hybrid scheduling, current research focuses on forbidden zone avoidance to mitigate their impact on the system's economic performance [13], reliability [14], and flexibility [15].

In this paper, instead of modeling the off-design zone as a forbidden zone where no operation is allowed, we propose a novel approach to determine the conditions under which the turbine can occasionally operate within the off-design zones, aligning with real-world circumstances. We introduce operating zones associated with various production costs derived from the fatigue analysis of the hydraulic turbine and calculate them based on the turbine replacement cost. These costs are then incorporated into a short-term hybrid scheduling tool based on Mixed Integer Linear Programming (MILP). Including production costs in the optimization problem helps avoid the high-cost zone and shifts the working point to a low-cost zone. However, operation in a high-cost zone can be justified if the short-term profit from selling power to the market outweighs the cost associated with potential turbine damage. Therefore, the resulting operational pattern considers not only short-term economic factors such as day-ahead market prices and water value but also lifetime hydraulic turbine cost, leading to a more comprehensive scheduling plan. To the best of our knowledge, this paper is the first to include the lifetime hydraulic turbine cost in the short-term scheduling problem and to propose the concept of production costs for modeling off-design zones.

Furthermore, this paper addresses hybrid scheduling, integrating hydropower with floating solar photovoltaics (FPV). FPV, a promising application of PV modules, has gained global interest in recent years, especially when combined with hydropower [16]. Installed on the reservoir surface, FPV eliminates the need for additional land and shares electrical infrastructure and grid connection with the hydropower plant [17]. Additionally, FPV systems reduce reservoir evaporation and enhance PV panel efficiency by lowering the panels' operating temperature [18]. The synergy between solar and hydro energies offers complementary benefits, balancing seasonal inflow variations with solar energy fluctuations [19]. Africa, in particular, shows significant potential for hydro-FPV hybrid power plants, with simulations indicating up to a 58% increase in power output when FPV covers 1% of the reservoir surface [20].

This paper makes three key contributions: (1) It quantifies the accumulated damage in terms of production cost; (2) it includes the production cost in the short-term hybrid scheduling model; and (3) it proposes a method that considers the trade-off between the market price and hydraulic turbine cost when determining the optimal production schedules.

The remainder of the paper is structured as follows: In the next section, we propose the heuristics for converting the nonlinear accumulated damage associated with the hydraulic turbine cost into stepwise production costs that cover the entire operating range of the turbine. Section 3 presents the mathematical formulations that include the production costs

in a short-term hybrid scheduling model. Section 4 analyzes the impact of production costs on production schedules under four scenarios. The final section concludes the study.

2. Heuristics

This section introduces the heuristics of converting the nonlinear accumulated damage to stepwise production costs.

Each point in Figure 1 signifies the probability of a hydraulic turbine being entirely decommissioned after one week of continuous operation at a specified power output. These points are derived from measurements on prototypes using strain gauges positioned near areas of anticipated peak stress. Data are collected for each load condition as the turbine load varies from minimum to maximum. These data are then processed using standard cycle counting techniques and fatigue data for high-grade stainless steel. This process enables a typical fatigue analysis, resulting in the creation of Figure 1. Detailed methods for assessing fatigue can be found in [21].

The dashed line in Figure 1 represents the average probability of accumulated damage, denoted as $d(p)$. The reciprocal of this function, $d(p)^{-1}$, indicates the number of weeks the turbine can operate at output p before it is completely damaged, rendering the turbine's value C^{Turb} (USD) zero. We define the production cost $C^{\text{Prod}}(p)$ (USD/MWh) as the total depreciation of the turbine, as expressed in Equation (1). It should be noted that a week consists of 168 h, and the production cost varies with the operating point.

$$C^{\text{Prod}}(p) = \frac{C^{\text{Turb}}}{168 \cdot d(p)^{-1} \cdot p}. \tag{1}$$

The hybrid scheduling model used in this paper is a MILP problem. It is an operational tool many Nordic hydropower producers use for daily operations [22]. Any new functionality implemented should be consistent with the methodology of the original model. It ensures the continuity and consistency of the model's application in the real world. Therefore, we need to transfer the nonlinear and nonconvex Equation (1) into a linear function.

We outline the process for determining the stepwise linear production costs from an existing fatigue analysis, as depicted in Figure 1.

2.1. Step 1: Calculate the Accumulated Damage

We first equally divide the operating range from the minimum output of 3 MW to the maximum output of 45 MW, with an interval of 2 MW. The corresponding accumulated damage $d(p_x)$ for each power output p_x is calculated and represented in Figure 3a on a logarithmic scale (similar to Figure 1) and in Figure 3b on a linear scale. Figure 3b shows a higher probability of damage when the turbine operates within a specific zone, i.e., 17–27 MW.
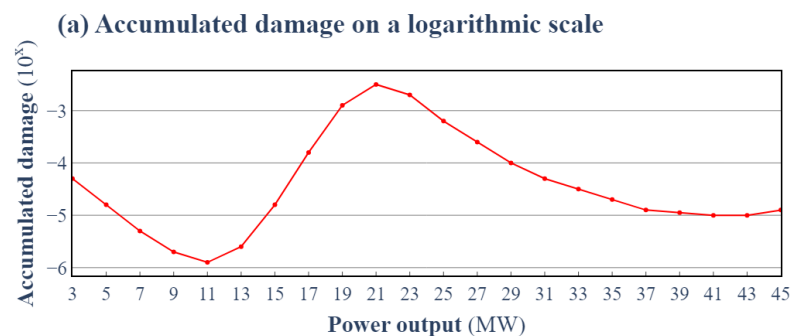

(a) Accumulated damage on a logarithmic scale

Figure 3. *Cont.*

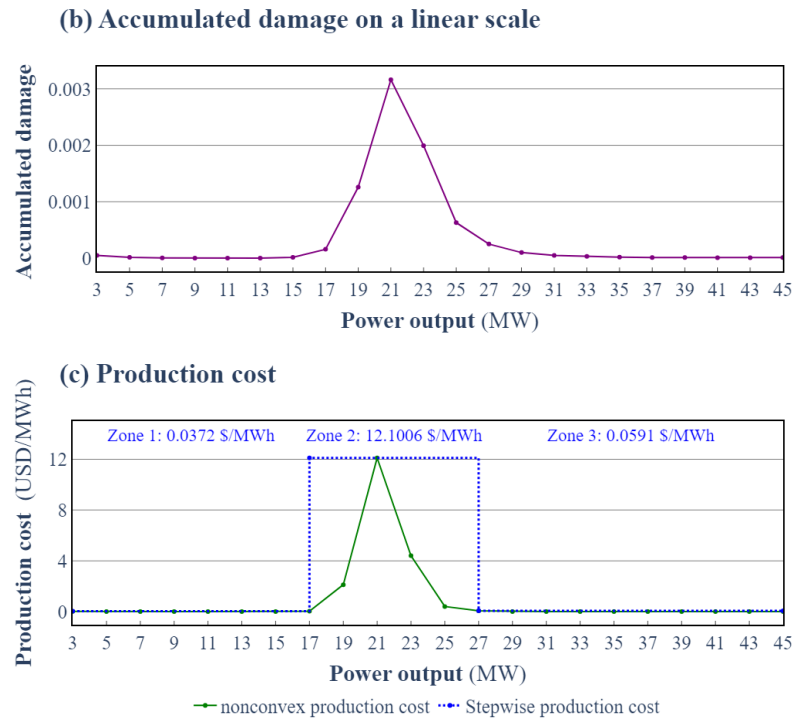**(b) Accumulated damage on a linear scale**

(c) Production cost

Figure 3. Conversion of nonlinear accumulated damage to stepwise linear production cost.

2.2. Step 2: Normalize the Accumulated Damage

We linearly normalize the accumulated damage to a value between 0 and 1. As shown in Table 1, the lowest damage $\underline{d(p)}$ is 1.26×10^{-6} when the power output is 11 MW; hence, it is normalized as 0. The maximum damage $\overline{d(p)}$ is 3.16×10^{-3} when the production is 21 MW and normalized as 1. Other values are standardized through Equation (2). This normalization facilitates a scalable comparison of the accumulated damage across the entire range of power outputs.

$$d(p_x)^{\text{NORM}} = \frac{d(p_x) - \underline{d(p)}}{\overline{d(p)} - \underline{d(p)}}. \tag{2}$$

Table 1. Calculation table for stepwise production cost.

Power Output (MW) p_x	Average Accumulated Damage (100%/week) $d(p_x)$	Reciprocal of Accumulated Damage (week) $d(p_x)^{-1}$	Normalized Accumulated Damage (100%/week) $d(p_x)^{\text{NORM}}$	Nonconvex Production Cost (USD/MWh) $C^{\text{Prod}}(p_x)$	Stepwise Production Cost (USD/MWh) $C_z^{\text{Prod}}[\underline{P}_{-z}, \overline{P}_z]$
3	5.01×10^{-5}	19,953	0.0155	0.0208	
5	1.58×10^{-5}	63,096	0.0046	0.0012	
7	5.01×10^{-6}	199,526	0.0012	0.0001	
9	2.00×10^{-6}	501,187	0.0002	0.0000	0.0373
11	1.26×10^{-6}	794,328	0.0000	0.0000	
13	2.51×10^{-6}	398,107	0.0004	0.0000	
15	1.58×10^{-5}	63,096	0.0046	0.0004	
17	1.58×10^{-4}	6310	0.0497	0.0373	
19	1.26×10^{-3}	794	0.3979	2.1184	
21	3.16×10^{-3}	316	1.0000	12.1006	12.1006
23	2.00×10^{-3}	501	0.6308	4.3974	
25	6.31×10^{-4}	1585	0.1992	0.4040	
27	2.51×10^{-4}	3981	0.0791	0.0591	

Table 1. *Cont.*

Power Output (MW) p_x	Average Accumulated Damage (100%/week) $d(p_x)$	Reciprocal of Accumulated Damage (week) $d(p_x)^{-1}$	Normalized Accumulated Damage (100%/week) $d(p_x)^{\mathrm{NORM}}$	Nonconvex Production Cost (USD/MWh) $C^{\mathrm{Prod}}(p_x)$	Stepwise Production Cost (USD/MWh) $C_z^{\mathrm{Prod}}[\underline{P}_z,\overline{P}_z]$
29	1.00×10^{-4}	10,000	0.0312	0.0087	
31	5.01×10^{-5}	19,953	0.0155	0.0020	
33	3.16×10^{-5}	31,623	0.0096	0.0007	
35	2.00×10^{-5}	50,119	0.0059	0.0003	
37	1.26×10^{-5}	79,433	0.0036	0.0001	0.0591
39	1.12×10^{-5}	89,125	0.0032	0.0001	
41	1.00×10^{-5}	100,000	0.0028	0.0001	
43	1.00×10^{-5}	100,000	0.0028	0.0001	
45	1.26×10^{-5}	79,433	0.0036	0.0001	

2.3. Step 3: Compute the Nonconvex Production Cost

We assume a typical Kaplan turbine costs 300,000 USD/MW multiplied by its maximum power output (MW) [23]. Consequently, the turbine cost C^{Turb} in this example is 13,500,000 USD (=300,000 × 45). We further assume that operating at the point with the highest accumulated damage will result in the complete depreciation of the turbine, whereas operating at the point with the lowest accumulated damage will incur no cost. As a result, the continuous production cost in Equation (1) becomes discrete $C^{\mathrm{Prod}}(p_x)$, as expressed in Equation (3).

$$C^{\mathrm{Prod}}(p_x) = \frac{d(p_x)^{\mathrm{NORM}} \cdot C^{\mathrm{Turb}}}{168 \cdot d(p_x)^{-1} \cdot p_x}. \tag{3}$$

The fifth column in Table 1 enumerates the production cost for each output, and these values are plotted in green in Figure 3c. The nonconvex production cost curve keeps a similar shape to the accumulated damage on a linear scale (Figure 3b). However, the value and unit differ since power output and turbine cost are considered.

2.4. Step 4: Determine the Stepwise Linear Production Cost

The last heuristic we adopt is to divide the production range into three zones: [3, 17], [17, 27], and [27, 45]. The highest production cost in each zone $C_z^{\mathrm{Prod}}[\underline{P}_z, \overline{P}_z]$ is defined as the constant production cost for that zone, as depicted by the blue dotted line in Figure 3c. While it is a relatively conservative approach to defining the production cost, it is reasonable to associate a slightly higher cost with the accumulated damage. Frequent turbine failure could increase inventory and repair costs. If such failures occur when solar generation is low, energy may need to be purchased at higher market prices to fulfill load obligations. Hence, all these costs should be considered to establish the validity of the production cost.

3. Mathematical Formulations

This section first presents the basic mathematical formulations of the short-term hybrid scheduling problem based on the Short-term Hybrid Optimization Program (SHOP). Then, we explain the modifications to the model when the operating zones associated with production costs are included.

SHOP, developed by SINTEF Energy Research, is a scheduling tool that considers complex watercourses, technical details of the production system, and various strategic, regulatory, and market constraints. Many Nordic hydropower producers use SHOP for their daily operations. The solution algorithm in SHOP is decomposed into unit commitment (UC) mode and unit load dispatch (ULD) mode. In the UC mode, a MILP model is resolved to specify each unit's on/off status per period. Iterations are conducted to stabilize the

water level variation in the reservoirs. The convergence criterion in UC mode is usually achieved after three to five iterations. Subsequently, the binary variables are fixed in the ULD mode, transforming the model into a pure LP problem. A dispatch schedule is determined, providing the exact generation for each committed unit. For a detailed explanation of the solution methodology of SHOP, interested readers are referred to [22].

3.1. Sets and Indexes

T	Set of time periods, index $t \in T$.
K	Set of reservoirs, index $k \in K$.
U_k	Set of all direct upstream hydraulic objects for reservoir k, index $u \in U_k$.
O_k	Set of FPVs that is installed on the surface of reservoir k, index $o \in O_k$.
J	Set of rivers, index $j \in J$.
S	Set of hydropower plants, index $s \in S$.
I_s	Set of units in hydropower plant s, index $i \in I_s$.
Z_i	Set of operating zones of unit i, index $z \in Z_i$.

3.2. Parameters

$\bar{t}$	Number of the periods of the scheduling problem.
ΔT	Length of each period (hour, h).
$V_{k,0}$	Initial water storage of reservoir k (million m^3).
$\underline{V}_k, \overline{V}_k$	The minimum and maximum water volume of reservoir k (million m^3).
$\underline{Q}_{j,t}^{\text{River}}$	The minimum flow requirement of river j in period t (m^3/s)
$\underline{P}_{i,s}^{\text{Hydro}}, \overline{P}_{i,s}^{\text{Hydro}}$	The minimum and maximum power output of unit i in hydropower plant s (MW).
$\underline{P}_{z,i,s}^{\text{Hydro}}, \overline{P}_{z,i,s}^{\text{Hydro}}$	The lower and upper bounds of output in operating zone z of unit i in plant s (MW).
$\underline{Q}_{i,s,t}, \overline{Q}_{i,s,t}$	The minimum and maximum water discharge of unit i in plant s in period t (m^3/s).
$\underline{Q}_{z,i,s,t}, \overline{Q}_{z,i,s,t}$	The lower and upper bounds of discharge in operating zone z of unit i in hydropower plant s in period t (m^3/s).
$\Omega_{i,s,0}$	Initial status of unit i in hydropower plant s (1 on, 0 off).
$\overline{P}_{o,t}^{\text{Solar}}$	Forecasted solar power production of FPV o in period t (MW).
M_t^{Sell}	Market price for selling energy in period t (USD/MWh).
$W_{k,\bar{t}}^{\text{End}}$	Marginal water value of reservoir k at the end of the scheduling horizon $\bar{t}$ (USD/MWh).
γ_s	Energy conversion factor for hydropower plant s (MWh/million m^3).
$C_{i,s,t}^{\text{Start}}$	Start-up cost of unit i in hydropower plant s in period t (USD).
$C_{z,i,s,t}^{\text{Prod}}$	Production cost in operating zone z of unit i in hydropower plant s (USD/MWh).
$C_{o,t}^{\text{Solar}}$	Curtailment cost of FPV o in period t (USD/MWh).
C_t^{Load}	Penalty cost for failing to deliver load obligation in period t (USD/MWh).
C_t^{Flow}	Penalty cost for breaking the minimum flow requirement of river j in period t (USD/m^3/s).
P_t^{Load}	Load obligation in period t (MW).

3.3. Variables

$\omega_{i,s,t} \in \{0,1\}$	Status of unit i in hydropower plant s in period t (1 on, 0 off).
$\varphi_{z,i,s,t} \in \{0,1\}$	Status of unit i in hydropower plant s in period t ($\varphi_{z,i,s,t} = 1$ if the unit is operated in zone z, 0 otherwise).
$\mu_{i,s,t} \in \{0,1\}$	Start-up decision of unit i in hydropower plant s in period t (1 if the unit is started up in period t, 0 otherwise).
$v_{k,t}$	Water volume of reservoir k at the end of period t (million m^3).
$q_{k,t}^{\text{Inflow}}$	Actual inflow into reservoir k in period t (m^3/s).

$q_{u,t}^{\text{Up}}$	Regulated water release from upstream hydraulic object u to reservoir k in period t (m^3/s).
$q_{k,t}^{\text{Bypass}}$	Water discharged from reservoir k through bypass gate in period t (m^3/s).
$q_{i,s,t}^{\text{Hydro}}$	Water discharge of unit i in hydropower plant s in period t (m^3/s).
$q_{z,i,s,t}^{\text{Hydro}}$	Water discharge in operating zone z of unit i in hydropower plant s in period t (m^3/s).
$p_{i,s,t}^{\text{Hydro}}$	Hydropower output of unit i in hydropower plant s in period t (MW).
$p_{z,i,s,t}^{\text{Hydro}}$	Hydropower output in operating zone z of unit i in hydropower plant s in period t (MW).
$p_{o,t}^{\text{Solar}}$	Solar power output of FPV o in period t (MW).
p_t^{Sell}	Power sold to the market in period t (MW).
n_t^{Load}	Unfulfilled load amount in period t (MW).
$n_{j,t}^{\text{Flow}}$	Unfulfilled minimum flow amount of river j in period t (m^3/s).

3.4. Objective Function

The objective function in Equation (4) is to maximize the net revenue derived from two sources: (1) energy sold in the day-ahead market during the scheduling horizon and (2) water preserved in the reservoirs at the end of the scheduling period. In a hydro-dominant scheduling problem, the optimal production decision is significantly influenced by the trade-off between the market price M_t^{Sell} and the water value $W_{k,\bar{t}}^{\text{End}}$. The cost component of the equation comprises the start-up cost of hydro units, solar curtailment cost, and penalty costs incurred due to non-compliance with load obligations and violations of minimum flow constraints in the river. The load income is not included in the objective function since it is a fixed sum in a deterministic model and is calculated post-optimization.

$$\max\left(\sum_{t\in T} M_t^{\text{Sell}}\cdot\Delta T\cdot p_t^{\text{Sell}} + \sum_{k\in K} W_{k,\bar{t}}^{\text{End}}\cdot\gamma_s\cdot v_{k,\bar{t}} - \sum_{t\in T}\sum_{s\in S}\sum_{i\in I_s} C_{i,s,t}^{\text{Start}}\cdot\mu_{i,s,t} \right.$$
$$\left. - \sum_{t\in T}\sum_{o\in O} C_{o,t}^{\text{Solar}}\cdot\Delta T\cdot n_{o,t}^{\text{Solar}} - \sum_{t\in T} C_t^{\text{Load}}\cdot\Delta T\cdot n_t^{\text{Load}} - \sum_{t\in T}\sum_{j\in J} C_{j,t}^{\text{Flow}}\cdot n_{j,t}^{\text{Flow}} \right). \tag{4}$$

3.5. Related Constraints

3.5.1. Power Balance Constraint

Power generated from hydro and FPV should primarily meet the load obligations. Surplus power can be sold to the market.

$$\sum_{s\in S}\sum_{i\in I_s} p_{i,s,t}^{\text{Hydro}} + \sum_{o\in O} p_{o,t}^{\text{Solar}} - p_t^{\text{Sell}} + n_t^{\text{Load}} = P_t^{\text{Load}}, \quad \forall t\in T. \tag{5}$$

3.5.2. Solar Power Production Constraint

The actual FPV generation should be restricted within the forecast. The curtailed solar power is incorporated in the objective function associated with the curtailment cost.

$$p_{o,t}^{\text{Solar}} + n_{o,t}^{\text{Solar}} = \overline{P}_{o,t}^{\text{Solar}}, \quad \forall o\in O_k, k\in K, t\in T. \tag{6}$$

3.5.3. Reservoir-Related Constraints

Equations (7)–(10) represent the standard hydrological balance and storage limits of a cascaded reservoir k connected to plant s and downstream river j. The calculation of water evaporation leverages the solution algorithm of SHOP. Evaporation is deducted from the forecast inflow to account for the dynamic variations in the reservoir's surface area. Therefore, inflow $q_{k,t}^{\text{Inflow}}$ in water balance constraint (8) is a variable, not a fixed parameter. For details on incorporating evaporation in SHOP, refer to [24].

$$v_{k,0} = V_{k,0}, \quad \forall k\in K. \tag{7}$$

$$v_{k,t} = v_{k,t-1} + 0.0036 \cdot \Delta T \cdot \left(q_{k,t}^{\text{Inflow}} + \sum_{u \in U_k} q_{u,t}^{\text{Up}} - \sum_{i \in I_s} q_{i,s,t}^{\text{Hydro}} - q_{k,t}^{\text{Bypass}} \right), \ \forall k \in K, t \in T. \quad (8)$$

$$\underline{V}_k \leq v_{k,t} \leq \overline{V}_k, \ \ \forall k \in K, t \in T. \quad (9)$$

$$\sum_{i \in I_s} q_{i,s,t}^{\text{Hydro}} + q_{k,t}^{\text{Bypass}} + n_{j,t}^{\text{Flow}} \geq \underline{Q}_{j,t}^{\text{River}}, \ \ \forall j \in J, t \in T. \quad (10)$$

3.5.4. Hydropower Production Constraints

The hydropower production function in Equation (11) is a complex, state-dependent, nonlinear, and nonconvex function. Reference [22] provides details on transforming this function into a MILP setting. Equation (12) sets the power output limits of the generator, and Equation (13) specifies the discharge range of the turbine. Equations (14) and (15) reflect the unit's start-up decision based on the commitment status of the units during two consecutive periods.

$$p_{i,s,t}^{\text{Hydro}} = f\left(v_{k,t-1}, q_{i,s,t}^{\text{Hydro}} \right), \ \ \forall i \in I_s, s \in S, \ t \in T. \quad (11)$$

$$\underline{P}_{i,s}^{\text{Hydro}} \cdot \omega_{i,s,t} \leq p_{i,s,t}^{\text{Hydro}} \leq \overline{P}_{i,s}^{\text{Hydro}} \cdot \omega_{i,s,t}, \ \ \forall i \in I_s, s \in S, \ t \in T. \quad (12)$$

$$\underline{Q}_{i,s,t} \cdot \omega_{i,s,t} \leq q_{i,s,t}^{\text{Hydro}} \leq \overline{Q}_{i,s,t} \cdot \omega_{i,s,t}, \ \ \forall i \in I_s, s \in S, \ t \in T. \quad (13)$$

$$\omega_{i,s,0} = \Omega_{i,s,0}, \ \ \forall i \in I_s, s \in S. \quad (14)$$

$$\mu_{i,s,t} \geq \omega_{i,s,t} - \omega_{i,s,t-1}, \ \ \forall i \in I_s, s \in S, \ t \in T. \quad (15)$$

3.5.5. Modification After Including Production Cost

If operating zone z is introduced for unit i, production and discharge in Equation (11) are then calculated within each zone, i.e., $p_{i,s,t}^{\text{Hydro}}$ is replaced with $p_{z,i,s,t}^{\text{Hydro}}$, and $q_{i,s,t}^{\text{Hydro}}$ with $q_{z,i,s,t}^{\text{Hydro}}$. Equations (12)–(15) are correspondingly updated as Equations (16)–(19), and $\omega_{i,s,t}$ is replaced with $\varphi_{z,i,s,t}$. Note that $\underline{P}_{z,i,s}^{\text{Hydro}}$ and $\overline{P}_{z,i,s}^{\text{Hydro}}$ are the lower and upper bounds of power output in each zone, as defined in Section 2.

$$\underline{P}_{z,i,s}^{\text{Hydro}} \cdot \varphi_{z,i,s,t} \leq p_{z,i,s,t}^{\text{Hydro}} \leq \overline{P}_{z,i,s}^{\text{Hydro}} \cdot \varphi_{z,i,s,t}, \ \ \forall z \in Z_i, i \in I_s, s \in S, t \in T. \quad (16)$$

$$\underline{Q}_{z,i,s,t} \cdot \varphi_{z,i,s,t} \leq q_{z,i,s,t}^{\text{Hydro}} \leq \overline{Q}_{z,i,s,t} \cdot \varphi_{z,i,s,t}, \ \ \forall z \in Z_i, i \in I_s, s \in S, t \in T. \quad (17)$$

$$\sum_{z \in Z_i} \varphi_{z,i,s,0} = \Omega_{i,s,0}, \ \ \forall i \in I_s, s \in S. \quad (18)$$

$$\mu_{i,s,t} \geq \sum_{z \in Z_i} \varphi_{z,i,s,t} - \sum_{z \in Z_i} \varphi_{z,i,s,t-1}, \ \ \forall i \in I_s, s \in S, \ t \in T. \quad (19)$$

Equation (20) is added to ensure that, at most, one operating zone will be selected for each unit.

$$\sum_{z \in Z_i} \varphi_{z,i,s,t} \leq 1, \ \ \forall i \in I_s, s \in S, \ t \in T. \quad (20)$$

In the hydrological constraints (8) and (10), $\sum_{i \in I_s} q_{i,s,t}^{\text{Hydro}}$ is replaced by $\sum_{i \in I_s} \sum_{z \in Z_i} q_{z,i,s,t}^{\text{Hydro}}$. In the objective function, the sum of linear production cost $C_{z,i,s,t}^{\text{Prod}}$ multiplied by the corresponding production in each zone is subtracted from the total income. Equation (4) becomes

$$\max \left(\sum_{t \in T} M_t^{\text{Sell}} \cdot \Delta T \cdot p_t^{\text{Sell}} + \sum_{k \in K} W_{k,\bar{t}}^{\text{End}} \cdot \gamma_s \cdot v_{k,\bar{t}} - \sum_{t \in T} \sum_{s \in S} \sum_{i \in I_s} C_{i,s,t}^{\text{Start}} \cdot \mu_{i,s,t} - \sum_{t \in T} \sum_{o \in O} C_{o,t}^{\text{Solar}} \cdot \Delta T \cdot n_{o,t}^{\text{Solar}} - \right.$$
$$\left. \sum_{t \in T} C_t^{\text{Load}} \cdot \Delta T \cdot n_t^{\text{Load}} - \sum_{t \in T} \sum_{j \in J} C_{j,t}^{\text{Flow}} \cdot n_{j,t}^{\text{Flow}} - \sum_{t \in T} \sum_{s \in S} \sum_{i \in I_s} \sum_{z \in Z_i} C_{z,i,s,t}^{\text{Prod}} \cdot \Delta T \cdot p_{z,i,s,t}^{\text{Hydro}} \right). \tag{21}$$

As seen from the new objective function, since the production costs are associated with the hydraulic turbine cost and its accumulated damage, the optimization problem now considers not only the relationship between day-ahead market price and water value but also the lifetime hydraulic turbine cost.

4. Discussion

In this section, we generate four scenarios (S1–S4) and compare the impact of production costs on the operation pattern of the hydraulic turbine.

4.1. Physical Configurations of the Watercourse and FPV System

This case study is based on the construction plan for a hydro-FPV hybrid power plant project in Western Africa. The primary topology data of the watercourse can be found in Table 2. The cascaded hydro system includes two reservoirs and two hydropower plants, each equipped with two identical generating units, G1 and G2. The total hydropower production capacity is 126 MW. In scenarios that incorporate production costs, the operating zones are designated to both units in Plant B, which have the same turbine efficiency as shown in Figure 2. Environmental constraints imposed on hydropower plant operation are typically specified as minimum flow requirements for the downstream river, helping protect aquatic ecosystems. In this study, we assume a constant minimum flow. Although this is a simplified assumption, it is valid for short-term scheduling problems [25].

This study utilizes Ocean Sun's FPV system, which consists of multiple floaters connected side-by-side to form larger solar power installations. Each floater has a diameter of 75 m and a capacity of 0.65 MW_p (Megawatt peak) [26]. The FPV system is assumed to cover 0.5% of Reservoir A's maximum surface area. The number of floaters is calculated as follows:

$$\text{Number of floaters} = \frac{162 \times 0.5\%}{\pi \times (0.0375)^2} \approx 184. \tag{22}$$

This configuration results in a total installed peak PV power capacity of 120 MW_p, representing the maximum power output achievable by the FPV system under ideal sunlight and optimal conditions. During the chosen scheduling week, the forecasted maximum solar generation is 81.3 MW (the orange bar in Figure 4), which falls within the reasonable expected output range for the system. These one-week data are derived from a one-year FPV production dataset. Meteorological data from SolarGIS [27] were used as input parameters for simulations in PVsyst [28] to obtain hourly solar yield.
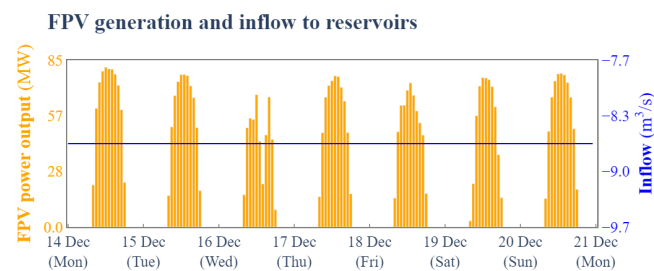

Figure 4. FPV generation and inflow to reservoirs.

Table 2. Topology data of the testing watercourse.

	Reservoir A	Reservoir B
Max volume (million m^3)	1169	12
Max surface area (km^2)	162	8
Max water level (m)	490	464
Min water level (m)	479	462
	Plant A	**Plant B**
Outlet line (m)	464	413
G1/G2 max power output (MW)	18	45
G1/G2 min power output (MW)	4	3
G1/G2 Start cost (USD)	10	10
	Downstream river	
Min flow (m^3/s)	30	
Penalty cost (USD/m^3/s)	1000	
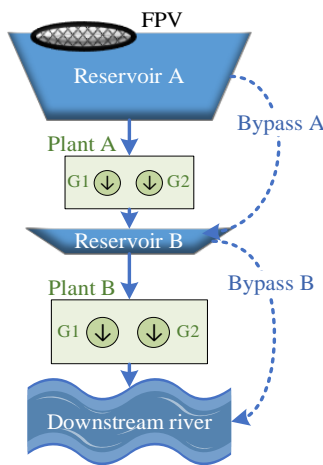
4.2. Scheduling Problem and Other Parameters

The scheduling period spans one week, with an hourly time resolution, starting from 00:00 on Monday, 14 December, and ending at 00:00 on Monday, 21 December. This period coincides with the dry season, with little inflow and an evaporation rate of 0.2 mm/h. The blue line in Figure 4 indicates the negative inflow due to evaporation.

In our previous work [29], we tested the impact of various energy pricing regimes on hybrid scheduling behavior. In this study, we adopt the day-ahead pricing regime derived from the day-ahead electricity market in the Southern African Power Pool [30]. We assume both reservoirs are full at the start of the scheduling period. The water value at the end of the scheduling period is set to be the mean of the hourly day-ahead market price, which is 130 USD/MWh. Both prices are depicted in Figure 5. The market price exhibits noticeable spikes during the morning and evening of working days and significantly diminishes over the weekend.

The baseload, the amount of power that must be delivered over a given period, is fixed at 100 MW from 7:00 to 22:00 daily. Any surplus electricity produced during this period can be sold at the day-ahead market price. The penalty for failing to meet the load obligation is 5000 USD/MWh.
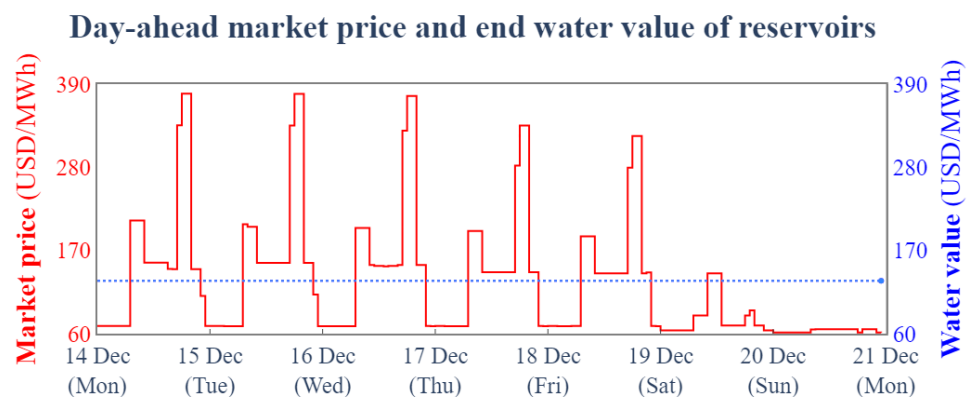
Figure 5. Day-ahead market price and end water value of reservoirs.

4.3. Scenario Description

Table 3 outlines the definition of the four scenarios. Scenario S1 is a standalone hydropower scheduling problem where neither production costs nor reserve obligations are considered. It serves as a reference case. In Scenario S2, FPV is added, transforming the scheduling problem into a hybridization of hydropower and solar power. Furthermore, in Scenario S3, operating zones associated with production costs are introduced to both generating units G1 and G2 in Plant B.

Table 3. Definition of four scenarios and their economic outcomes.

	Definition			Elements in Net Revenue (USD)						Net Revenue (USD)
	Energy Mix	Prod. Cost [a]	Reserve Oblig [b]	Energy Income	Load Income	Change in Water Value	Start Cost	Prod. Cost		
S1	Hydro alone	No	No	269,890	1,705,441	−1,759,953	220	/		215,158
S2	Hydro + Solar	No	No	725,724	1,705,441	−1,524,076	350	/		906,739
S3	Hydro + Solar	Yes	No	792,388	1,705,441	−1,590,996	280	419		906,134
S4	Hydro + Solar	Yes	20 MW	627,835	1,705,441	−1,497,510	260	13,700		821,806

[a] Prod. Cost is the abbreviation for "Production Cost". [b] Oblig is the abbreviation for "Obligation".

Finally, in Scenario S4, it is assumed that Plant_B_G1 is assigned to deliver a 20-MW Frequency Restoration Reserve for Up-regulation (FRR_UP). It implies that Plant_B_G1 must keep running to maintain synchronization with the electrical grid. Moreover, a minimum of 20 MW upward capacity should be reserved to ensure that, if up-regulation is required, Plant_B_G1 can increase its power generation from the current working point by 20 MW. Detailed formulations regarding the distribution of reserve obligations in SHOP are presented in [31].

All the scenarios are executed using SHOP v16.0.1 with CPLEX 20.1.0 as the solver. Both UC and ULD modes undergo three iterations. The calculation time for a single scenario runs between 2 and 5 s. No violations of load obligation, reserve obligation (if applicable), or flow constraints occur in any scenario. No solar power is curtailed.

4.4. Numerical Results

The economic outcomes of the four scenarios are delineated in Table 3. The energy income, start cost, and production cost correspond to the first, third, and last items in Equation (21), respectively. The load income is calculated by $\sum_{t \in T} M_t^{\text{Sell}} \cdot \Delta T \cdot P_t^{\text{Load}}$ and remains the same for all scenarios. To facilitate a uniform comparison of income and water value, we use the change in water value, as expressed in Equation (23), to indicate the decrease in water value in the reservoirs. Net revenue is the sum of the five elements mentioned above.

$$\sum_{k \in K} W_{k,\bar{t}}^{\text{End}} \cdot \gamma_s \cdot \left(v_{k,\bar{t}} - V_{k,0} \right). \tag{23}$$

The trajectory of Reservoir B is illustrated in Figure 6, while the weekly production schedules are presented in Figure 7. Overall, the addition of solar power in S2, S3, and S4, compared to the reference case of hydro alone (S1), enables more energy to be sold in the market. This leads to an augmentation in energy income and conservation of water in the reservoirs. On weekdays, hydropower production mirrors the market price trend, with increased power generation during periods of high prices. At weekends, when the price is low, hydropower and solar power co-production primarily meet the load obligation for peak hours. At night, at least one unit in Plant B remains operational to satisfy the minimum flow requirement of the downstream river.
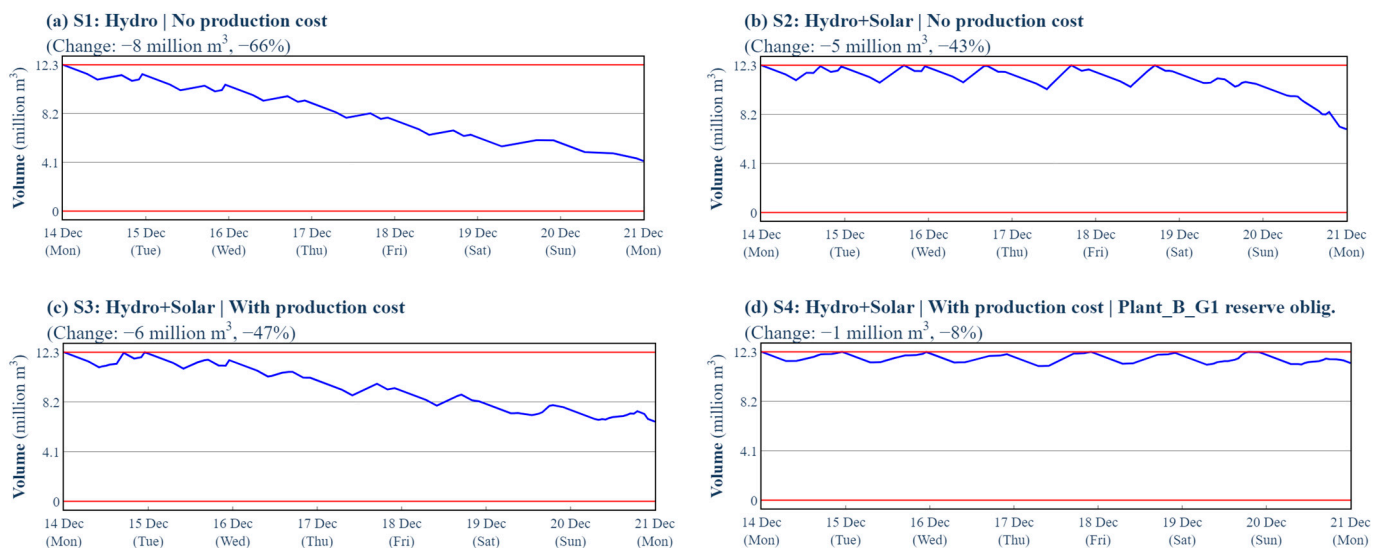
Figure 6. Reservoir B's trajectory of four scenarios.

Now, we focus on the production schedule on the weekend, Sunday (Figure 8), and the workday, Thursday (Figure 9), to examine the impact of production costs. Recall that three operating zones have been introduced to G1 and G2 in Plant B. The production cost associated with Zone 2 is the highest, i.e., 12.1006 USD/MWh, whereas the production costs for the other two zones are negligible, as explained in Section 2 and shown in Figure 3c. Therefore, operations in Zone 2 will be avoided in ordinary situations. The shifting of Plant_B_G1's working point from Zone 2 in S2 from 11:00 to 15:00 on Sunday (Figure 8b) to Zone 1 in S3 (Figure 8c) demonstrates the impact of production costs. To compensate for the reduction in power generation from Plant_B_G1 and meet the load obligation, Plant_A_G1 has to remain operational in S3. As operations in Zone 2 can be successively avoided, there are no significant changes in net revenue between S2 and S3, as shown in Table 3.

However, the trade-off becomes more intricate when the reserve obligation is allocated to Plant_B_G1. Given that Plant_B_G1 must reserve a minimum of 20 MW upward capacity, its maximum working point is reduced to 25 MW (=45−20), falling within the output range of Zone 2 [17,27]. Therefore, deciding whether to operate in Zone 1 to avoid high production costs or remain in Zone 2 to generate more power becomes challenging.

Take the optimal production schedules on Thursday in S4 as an example (Figure 9d). When the market price is close to the water value between 10:00 and 16:00, the working point is reduced to Zone 1. However, when the difference between the market price and water value can offset the production cost, i.e., 5:00–9:00 in the morning and 17:00–19:00 in the evening, Plant_B_G1 continues to operate in Zone 2. Additionally, Plant_B_G1 must operate in Zone 2 at 20:00 and 21:00 when the sun goes down to prevent breaking the load obligation. Consequently, S4 incurs high production costs since operation in Zone 2 cannot be avoided for some periods.

Based on the scenario comparisons, we can conclude that incorporating the lifetime hydraulic turbine cost into the short-term hybrid scheduling problem, in the form of operating zones associated with various production costs, has significant implications for economy and sustainability. Economically, this approach allows for optimized resource allocation. By avoiding high-cost zones when market prices are low and operating in those zones only when the short-term benefit outweighs the potential cost or when solar resources are unavailable, power producers can minimize operating time in off-design zones, thereby reducing the risk of premature turbine damage. In the long run, this strategic operation promotes safer plant operations and increases overall profitability.
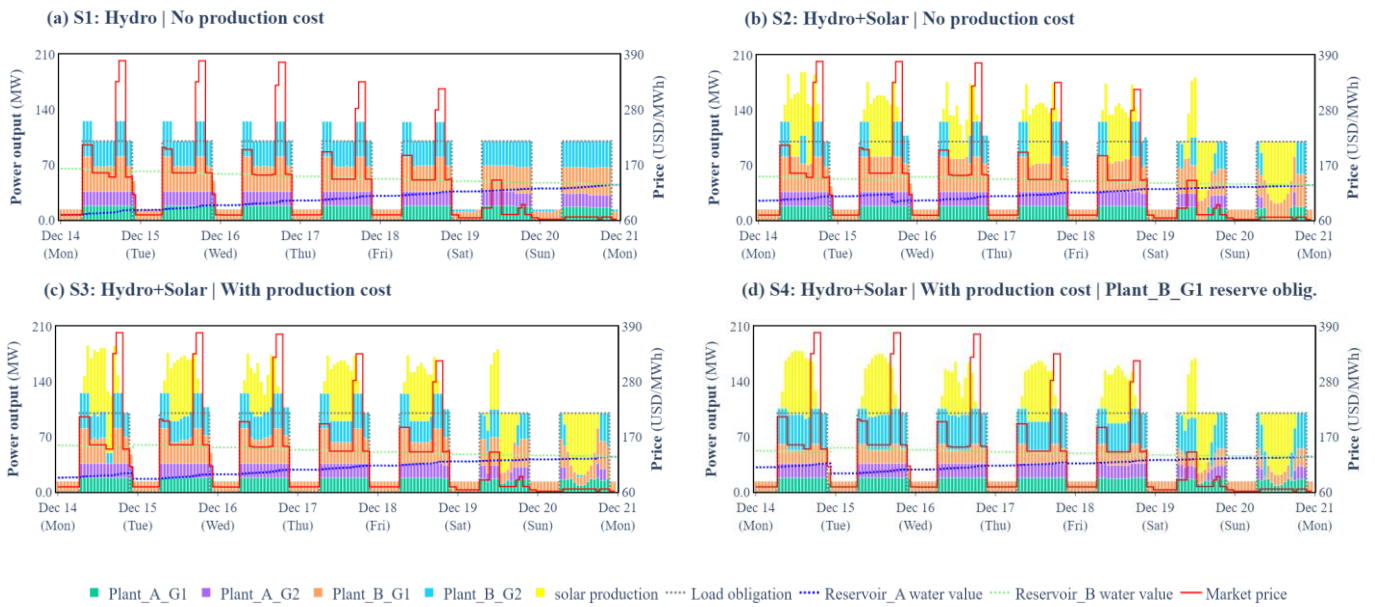
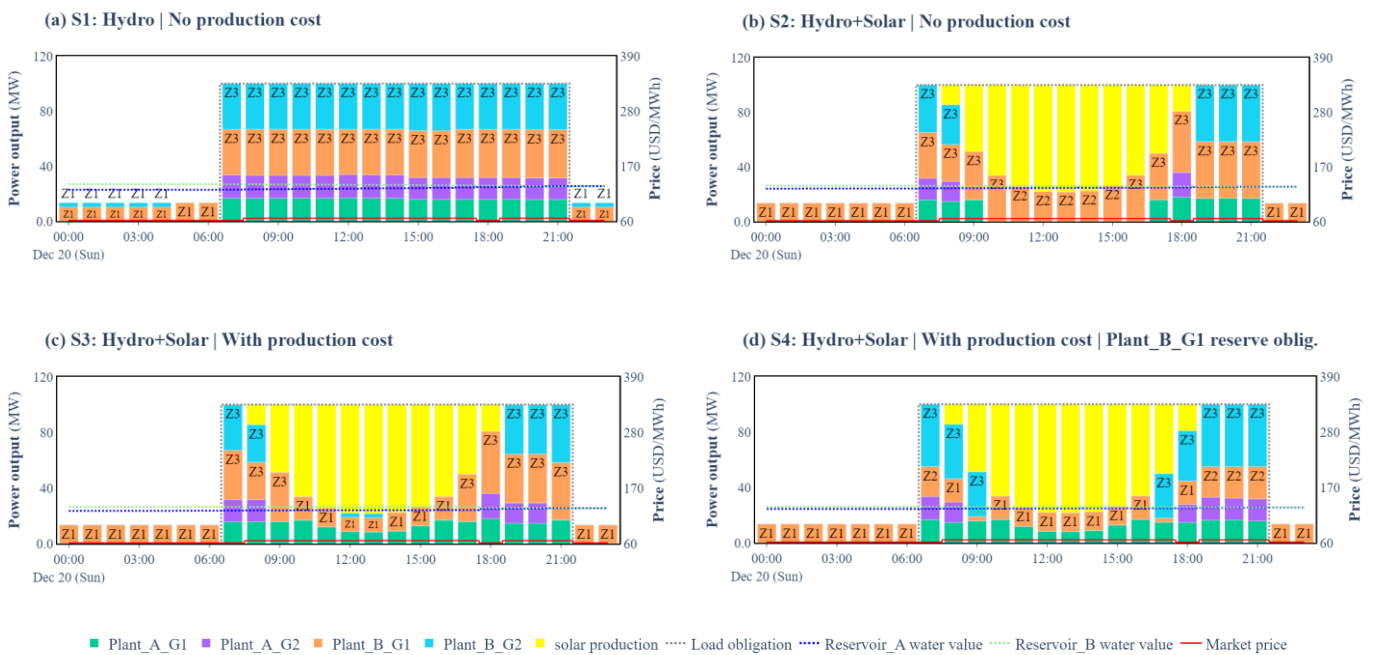**Figure 7.** Weekly production schedules of four scenarios.

Figure 8. Weekend production schedule (20 December 2015) of four scenarios.

From a sustainability perspective, minimizing operations in off-design zones reduces wear and tear on the turbine, leading to fewer maintenance requirements and extending the lifespan of the equipment. The balanced energy mix of hydro and solar ensures a more reliable energy supply, reducing dependency on a single energy source and enhancing the power system's resilience against climatic and operational variations.
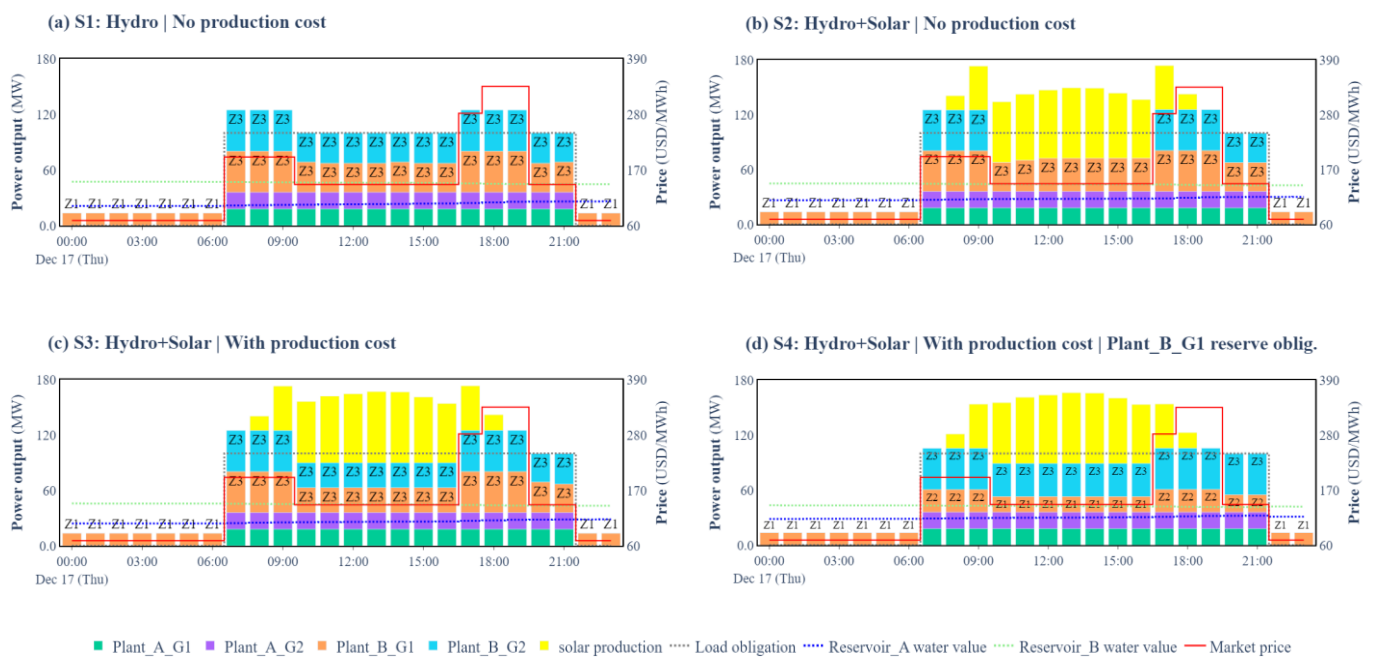
Figure 9. Weekday production schedule (17 December 2015) of four scenarios.

5. Conclusions

This paper presents a new method that permits the occasional and conditional operation in off-design zones, traditionally considered forbidden due to the increased risk of turbine damage. The main findings highlight that introducing operating zones associated with distinct production costs into a short-term hybrid scheduling model offers a more holistic scheduling plan that considers both short-term economic factors and lifetime hydraulic turbine costs. This approach can minimize the risk of premature turbine damage and optimize resource allocation.

The numerical results demonstrate that including the production cost in the hybrid scheduling problem alters the turbine's working point from a high-cost zone (12.1006 USD/MWh) to a low-cost zone (0.0372 USD/MWh). However, when the short-term profit (market price exceeding 200 USD/MWh and water value at 140 USD/MWh) is sufficient to cover the potential turbine damage loss (12.1006 USD/MWh) or when solar resources are unavailable, operation in the high-cost zone remains a feasible and valid option.

This study also has limitations. The heuristics used to transfer nonlinear accumulated damage to production costs represent a preliminary approach. We simplify the fatigue analysis by using the average probability of accumulated damage and dividing the entire operating range into three distinct zones. These heuristics are case- and model-dependent, necessitating more generalized and sophisticated methods. Future research could also incorporate an aging-dependent function to determine the maximum duration the hydraulic turbine can operate within the off-design zones and include it in the scheduling problem.

This research opens new avenues for future work, particularly in multi-energy complementary hybrid scheduling, and contributes significantly to the ongoing discourse on sustainable and efficient energy production. It emphasizes the importance of considering economic and operational factors in decision-making, ultimately leading to more flexible energy systems.

Conflicts of Interest: The authors declare no conflicts of interest. The funders had no role in the design of the study, in the collection, analysis, or interpretation of data, in the writing of the manuscript, or in the decision to publish the results.

References

1. Juras, J.; Canales, F.A.; Kies, A.; Guezgouz, M.; Beluco, A. A review on the complementarity of renewable energy sources: Concept, metrics, application and future research directions. *Sol. Energy* **2020**, *195*, 703–724. [CrossRef]
2. Li, X.D.; Yang, W.J.; Liao, Y.W.; Zhang, S.S.; Zheng, Y.; Zhao, Z.G.; Tang, M.J.; Cheng, Y.G.; Liu, P. Short-term risk-management for hydro-wind-solar hybrid energy system considering hydropower part-load operating characteristics. *Appl. Energy* **2024**, *360*, 122818. [CrossRef]
3. Chazarra, M.; Garcia-Gonzalez, J.; Perez-Diaz, J.I.; Arteseros, M. Stochastic optimization model for the weekly scheduling of a hydropower system in day-ahead and secondary regulation reserve markets. *Electr. Power Syst. Res.* **2016**, *130*, 67–77. [CrossRef]
4. Schäffer, L.E.; Korpås, M.; Bakken, T.H. Implications of environmental constraints in hydropower scheduling for a power system with limited grid and reserve capacity. In *Energy Systems*; Springer: Berlin/Heidelberg, Germany, 2023.
5. Doujak, E.; Stadler, S.; Fillinger, G.; Haller, F.; Maier, M.; Nocker, A.; Gassner, J.; Unterluggauer, J. Fatigue strength analysis of a prototype Francis turbine in a multilevel lifetime assessment procedure part I: Background, theory and assessment procedure development. *Energies* **2022**, *15*, 1148. [CrossRef]
6. Doujak, E.; Unterluggauer, J.; Fillinger, G.; Nocker, A.; Haller, F.; Maier, M.; Stadler, S. Fatigue strength analysis of a prototype Francis turbine in a multilevel lifetime assessment procedure part II: Method application and numerical investigation. *Energies* **2022**, *15*, 1165. [CrossRef]
7. Finardi, E.C.; Scuzziato, M.R. Hydro unit commitment and loading problem for day-ahead operation planning problem. *Int. J. Electr. Power Energy Syst.* **2013**, *44*, 7–16. [CrossRef]
8. Tong, B.; Zhai, Q.Z.; Guan, X.H. An MILP based formulation for short-term hydro generation scheduling with analysis of the linearization effects on solution feasibility. *IEEE Trans. Power Syst.* **2013**, *28*, 3588–3599. [CrossRef]
9. Guedes, L.S.M.; Maia, P.D.; Lisboa, A.C.; Gomes Vieira, D.A.; Saldanha, R.R. A unit commitment algorithm and a compact MILP model for short-term hydro-power generation scheduling. *IEEE Trans. Power Syst.* **2017**, *32*, 3381–3390. [CrossRef]
10. Jin, X.Y.; Liu, B.X.; Liao, S.L.; Cheng, C.T.; Zhao, Z.P.; Zhang, Y. Robust optimization for the self-scheduling and bidding strategies of a hydroproducer considering the impacts of crossing forbidden zones. *J. Water Resour. Plan. Manage.-ASCE* **2023**, *149*, 05022017. [CrossRef]
11. Cheng, C.T.; Wang, J.Y.; Wu, X.Y. Hydro unit commitment with a head-sensitive reservoir and multiple vibration zones using MILP. *IEEE Trans. Power Syst.* **2016**, *31*, 4842–4852. [CrossRef]
12. Su, C.G.; Yuan, W.L.; Cheng, C.T.; Wang, P.L.; Sun, L.F.; Zhang, T.H. Short-term generation scheduling of cascade hydropower plants with strong hydraulic coupling and head-dependent prohibited operating zones. *J. Hydrol.* **2020**, *591*, 125556. [CrossRef]
13. Jurasz, J.; Kies, A.; Zajac, P. Synergetic operation of photovoltaic and hydro power stations on a day-ahead energy market. *Energy* **2020**, *212*, 118686. [CrossRef]
14. Haoting, Q.; Tianzhi, L.; Jianhua, L.; Yunxia, W.; Hongtao, S. Optimal operation of cascaded hydropower plants in hydro-solar complementary systems considering the risk of unit vibration zone crossing. *Front. Energy Res.* **2023**, *11*, 1182614. [CrossRef]
15. Han, S.; Yuan, Y.F.; He, M.J.; Zhao, Z.W.; Xu, B.B.; Chen, D.Y.; Jurasz, J. A novel day-ahead scheduling model to unlock hydropower flexibility limited by vibration zones in hydropower-variable renewable energy hybrid system. *Appl. Energy* **2024**, *356*, 122379. [CrossRef]
16. Lee, N.; Grunwald, U.; Rosenlieb, E.; Mirletz, H.; Aznar, A.; Spencer, R.; Cox, S. Hybrid floating solar photovoltaics-hydropower systems: Benefits and global assessment of technical potential. *Renew. Energy* **2020**, *162*, 1415–1427. [CrossRef]
17. Kakoulaki, G.; Sanchez, R.G.; Amillo, A.G.; Szabo, S.; De Felice, M.; Farinosi, F.; De Felice, L.; Bisselink, B.; Seliger, R.; Kougias, I.; et al. Benefits of pairing floating solar photovoltaics with hydropower reservoirs in Europe. *Renew. Sust. Energ. Rev.* **2023**, *171*, 112989. [CrossRef]

18. Gadzanku, S.; Mirletz, H.; Lee, N.; Daw, J.; Warren, A. Benefits and Critical Knowledge Gaps in Determining the Role of Floating Photovoltaics in the Energy-Water-Food Nexus. *Sustainability* **2021**, *13*, 4317. [CrossRef]

19. Zhang, H.X.; Lu, Z.X.; Hu, W.; Wang, Y.T.; Dong, L.; Zhang, J.T. Coordinated optimal operation of hydro-wind-solar integrated systems. *Appl. Energy* **2019**, *242*, 883–896. [CrossRef]

20. Sanchez, R.G.; Kougias, I.; Moner-Girona, M.; Fahl, F.; Jager-Waldau, A. Assessment of floating solar photovoltaics potential in existing hydropower reservoirs in Africa. *Renew. Energy* **2021**, *169*, 687–699. [CrossRef]

21. Thibault, D.; Trudel, A. The IEC 63230: A new standard on the fatigue of hydraulic turbines to help the industry face the energy transition. Available online: https://www.researchgate.net/publication/375635581 (accessed on 30 August 2024).

22. Skjelbred, H.I.; Kong, J.; Fosso, O.B. Dynamic incorporation of nonlinearity into MILP formulation for short-term hydro scheduling. *Int. J. Electr. Power Energy Syst.* **2020**, *116*, 105530. [CrossRef]

23. AS, S.N. *Cost Base for Hydropower Plants (Over 10,000 kW)*; Norwegian Water Resources and Energy Directorate (NVE): Oslo, Norway, 2012; Available online: https://publikasjoner.nve.no/veileder/2012/veileder2012_03.pdf (accessed on 30 August 2024).

24. Kong, J.; Fjelldal, B.; Nøvik, H.; Engelstad, Ø.; Aasgård, E.K.; Trondsen, B.; Skjelbred, H.I. Impact of reservoir evaporation on determining power purchasing agreement under solar-hydro hybridization. In Proceedings of the 2023 4th International Conference on Clean and Green Energy Engineering (CGEE), Ankara, Turkiye, 26–28 August 2023.

25. Perez-Diaz, J.I.; Wilhelmi, J.R. Assessment of the economic impact of environmental constraints on short-term hydropower plant operation. *Energy Policy* **2010**, *38*, 7960–7970. [CrossRef]

26. Ocean Sun: Floating Solar Photovoltaics Producer. Available online: https://oceansun.no/our-products/ (accessed on 30 August 2024).

27. Data and Software Architects for Bankable Solar Investments. Available online: https://solargis.com/ (accessed on 30 August 2024).

28. Photovoltaic Software. Available online: https://www.pvsyst.com/ (accessed on 1 October 2023).

29. Kong, J.; Sheppard, A.J.; Nøvik, H.; Engelstad, Ø.; Fjelldal, B.; Klæboe, G.; Skjelbred, H.I. Impact of energy pricing regimes on production schedules under solar-hydro hybridization. In Proceedings of the 2023 IEEE International Conference on Environment and Electrical Engineering and 2023 IEEE Industrial and Commercial Power Systems Europe (EEEIC/I&CPS Europe), Madrid, Spain, 6–9 June 2023.

30. The Southern African Power Pool. Available online: https://www.sappmarket.com/ (accessed on 1 October 2023).

31. Kong, J.; Skjelbred, H.I. Operational hydropower scheduling with post-spot distribution of reserve obligations. In Proceedings of the 2017 14th International Conference on the European Energy Market (EEM), Dresden, Germany, 6–9 June 2017.